

Figure 1. Heating efficiency altitude profiles for ADM (black), *Richards* [2013] (orange), and *Rees et al.* [1992] (blue).

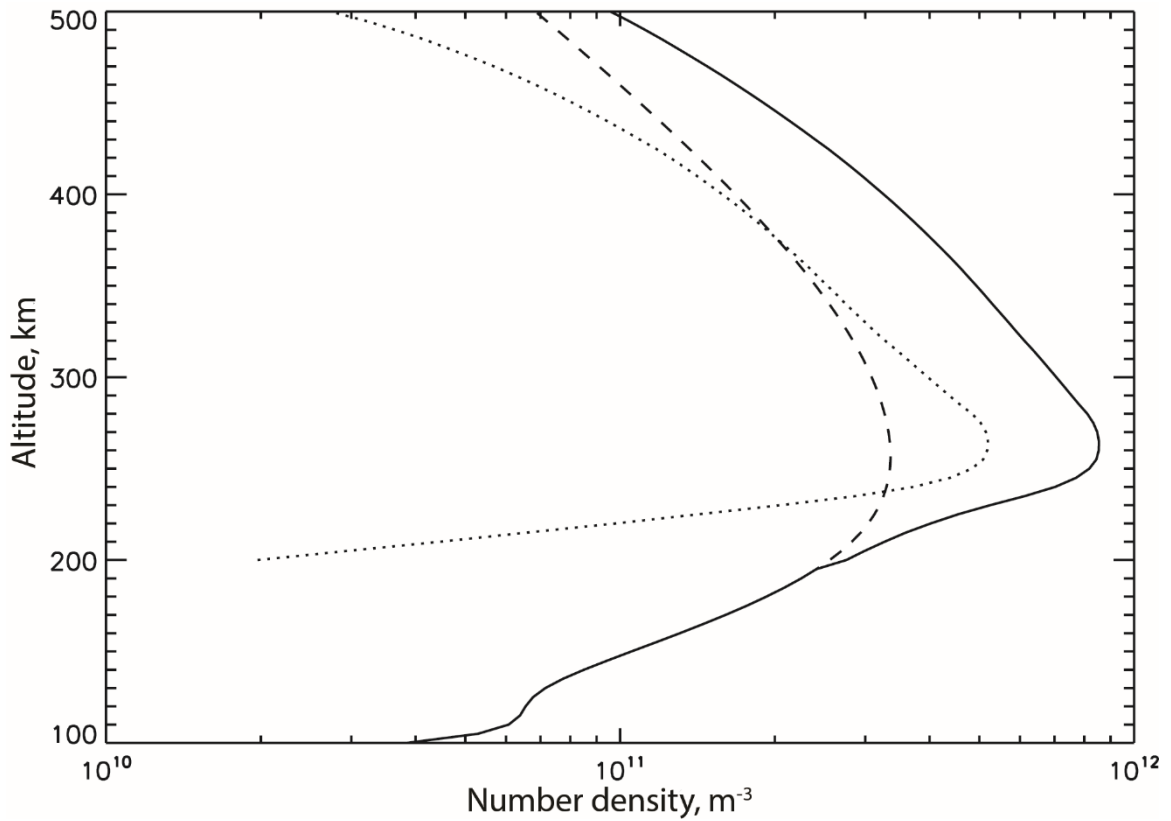


Figure 2. Electron density profiles for the background ionosphere (dashed), contribution due to particle precipitation (dotted) and the total (solid)

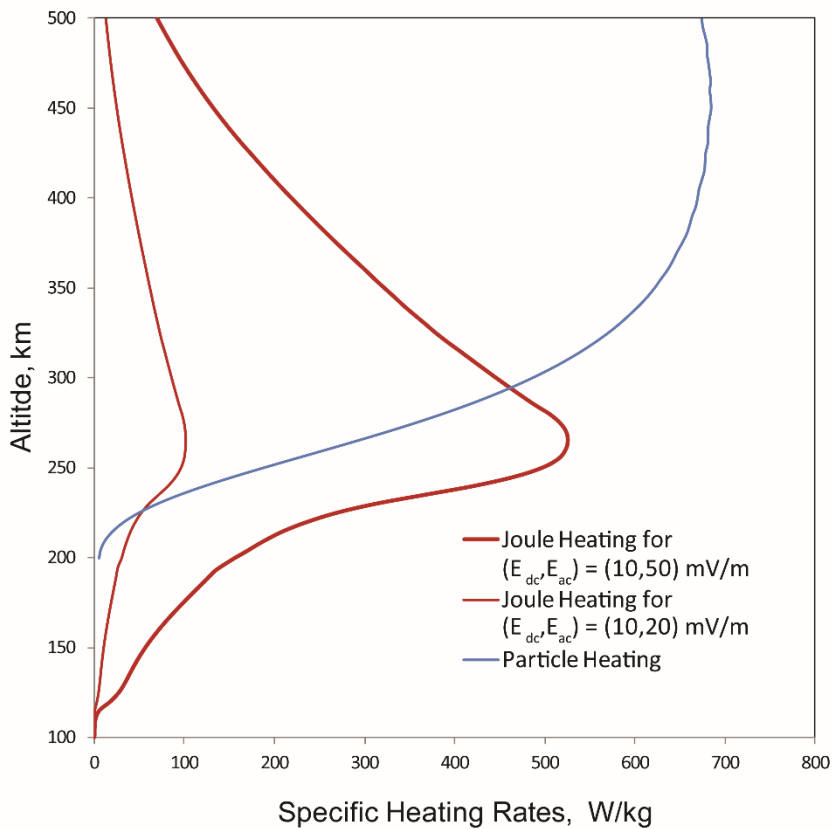
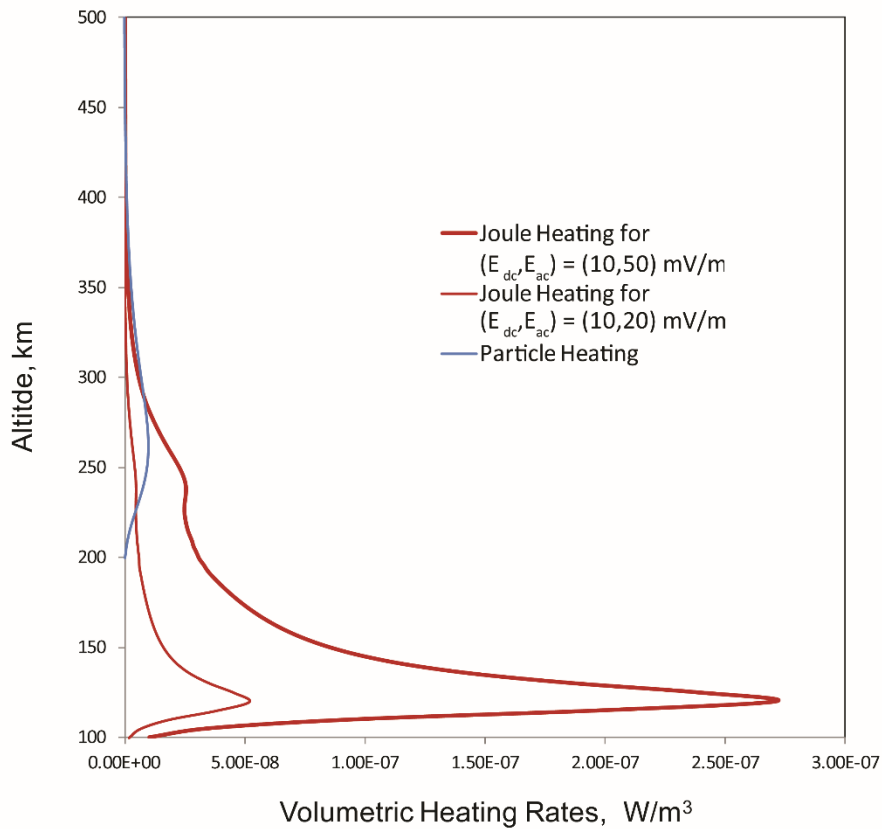


Figure 3. Volumetric heating rates (top) and specific heating rates (bottom) versus altitude for particle heating (blue curve) and Joule heating for two combinations of “dc” and “ac” electric fields.

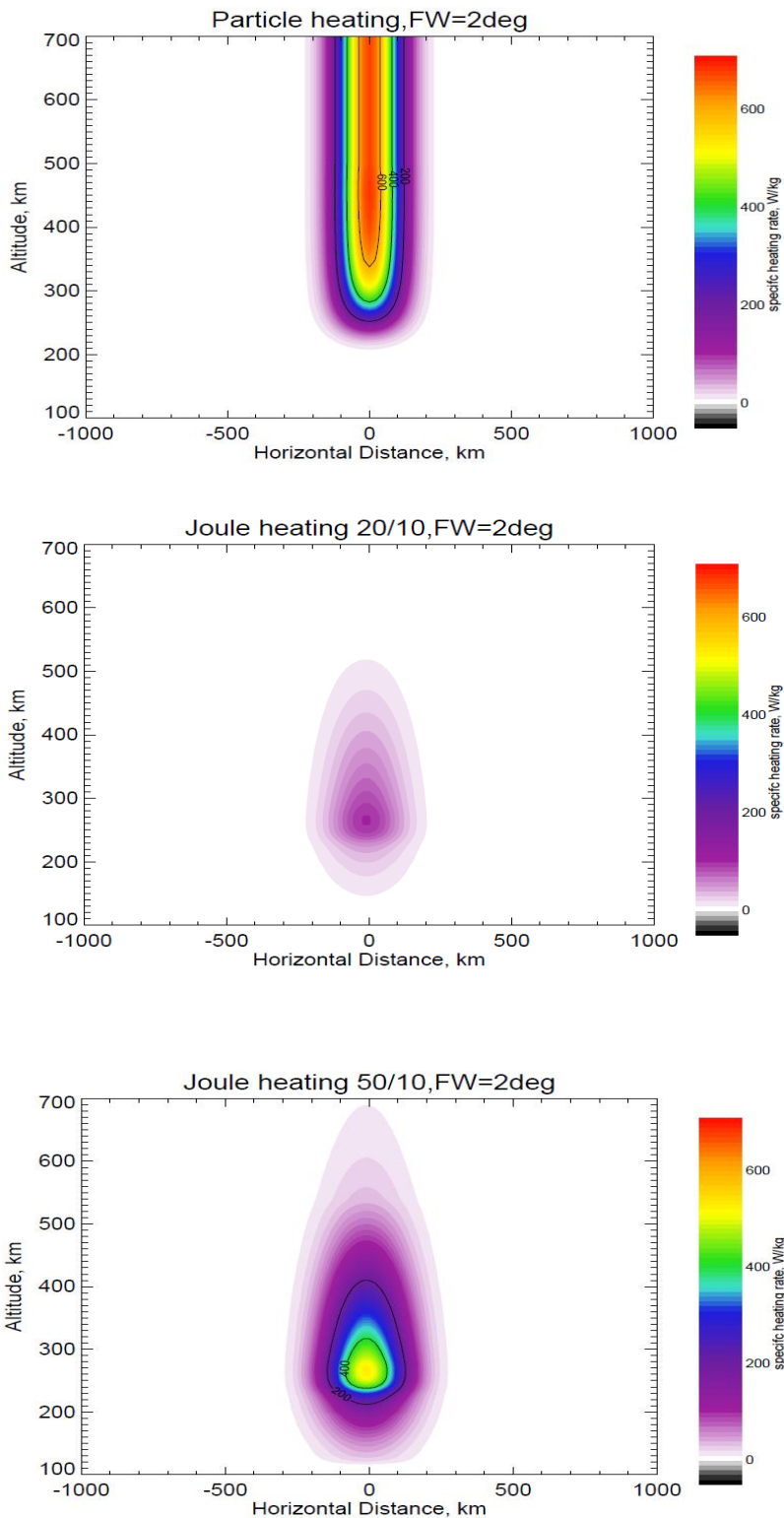


Figure 4. Specific heating rates as a function of altitude and distance from cusp center ( $2^\circ$  cusp width) for particle heating only case (top), E12 case (middle), and E15 case (bottom).

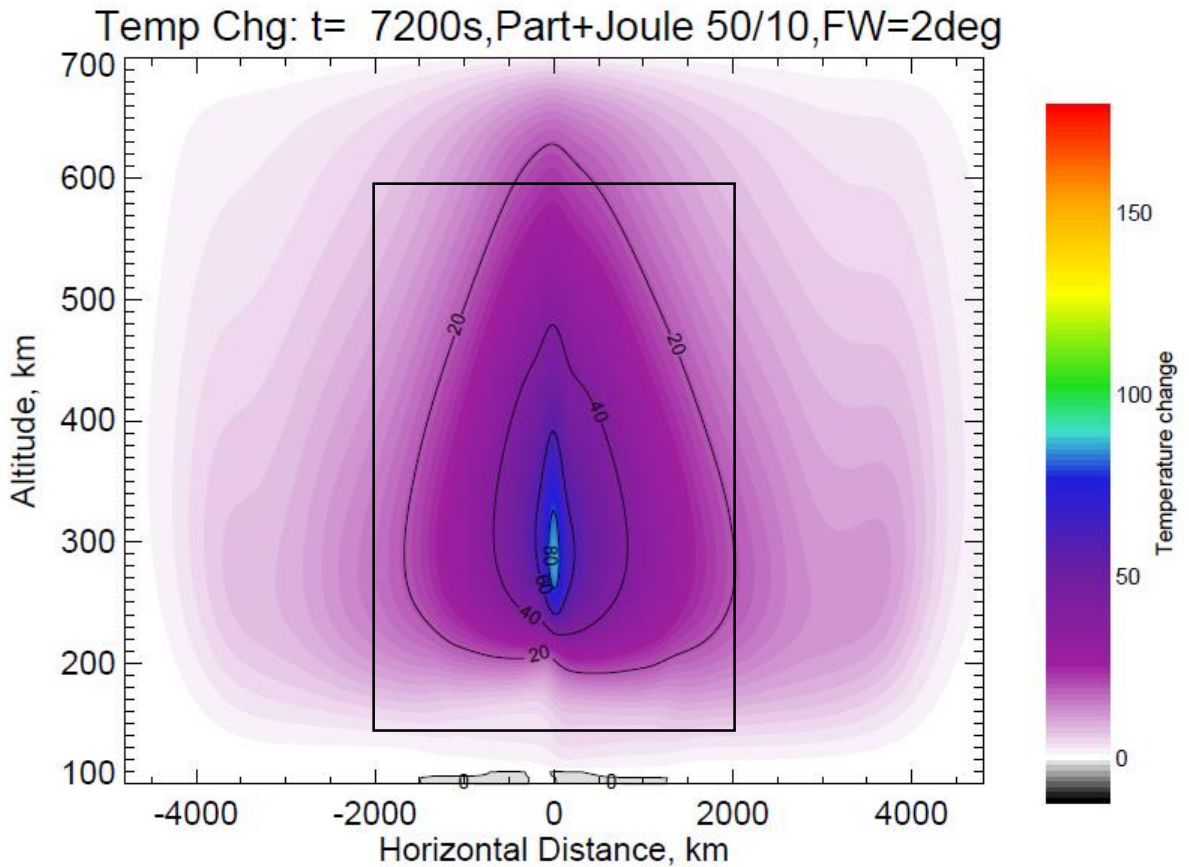


Figure 5. Temperature change at 7200 s over full computational domain for a cusp latitudinal  $e$ -folding width of  $2^\circ$  for case PEF2 heating.

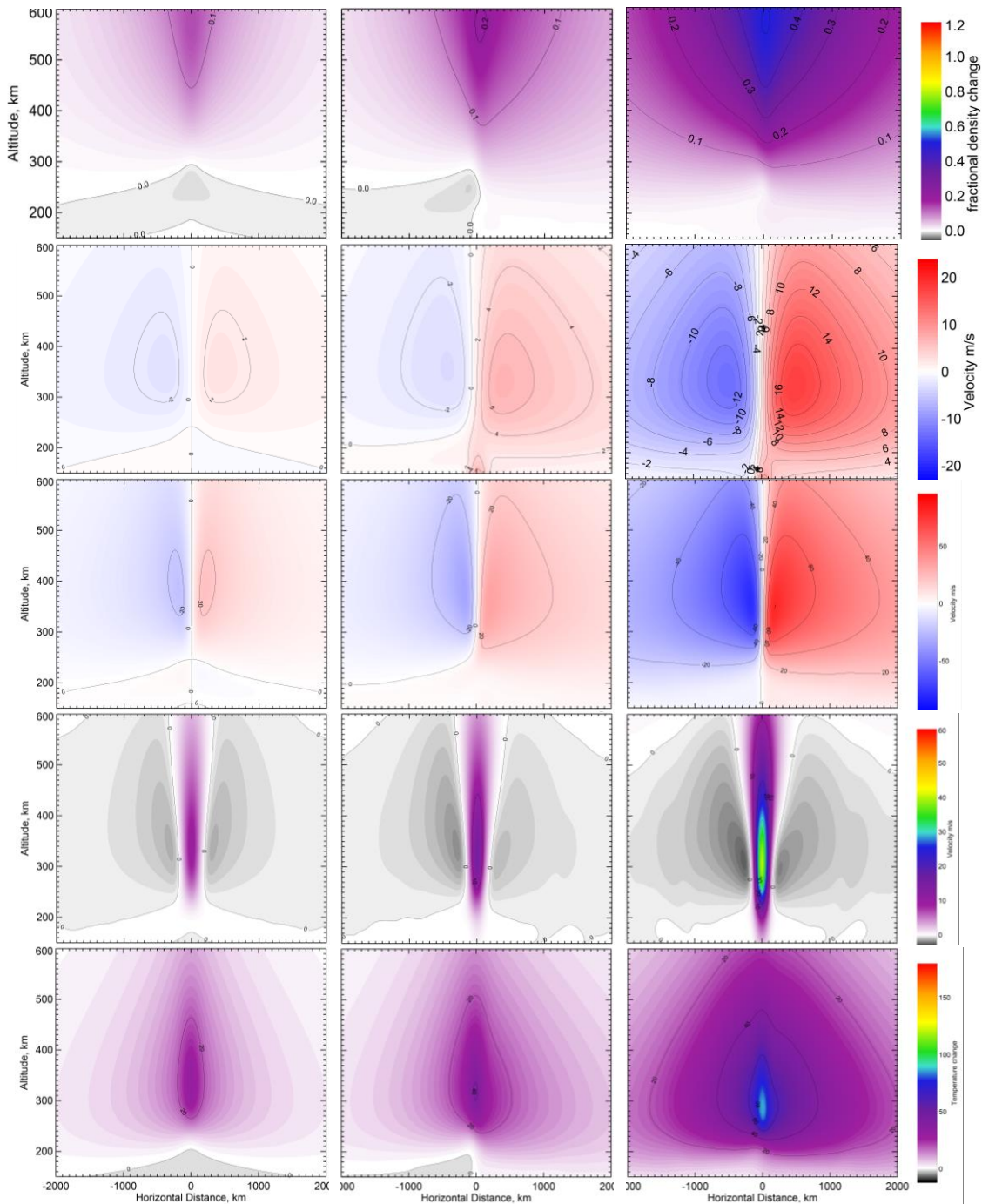


Figure 6. Fractional density change; zonal, meridional, and vertical winds; and temperature change at 7200 s for a cusp latitudinal e-folding width of  $2^\circ$  with heating due to (a) particle precipitation only corresponding to the PPO case, (b) particle precipitation and Joule heating corresponding to case PEF1 and (c) particle precipitation and Joule heating corresponding to case PEF2.

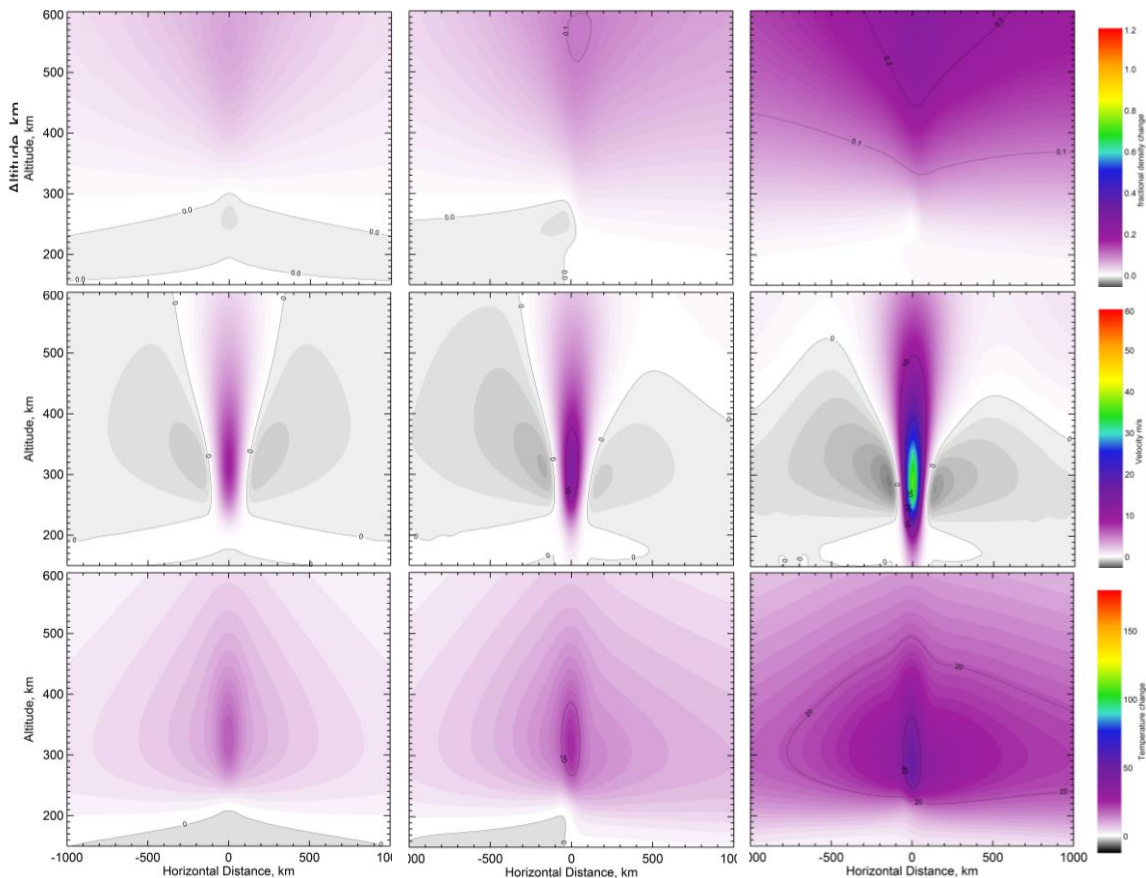


Figure 7. Fractional density change, vertical winds, and temperature change at 7200 s for a cusp latitudinal e-folding width of  $1^\circ$  with heating due to (a) particle precipitation only corresponding to the PPO case, (b) particle precipitation and Joule heating corresponding to case PEF1 and (c) particle precipitation and Joule heating corresponding to case PEF2.

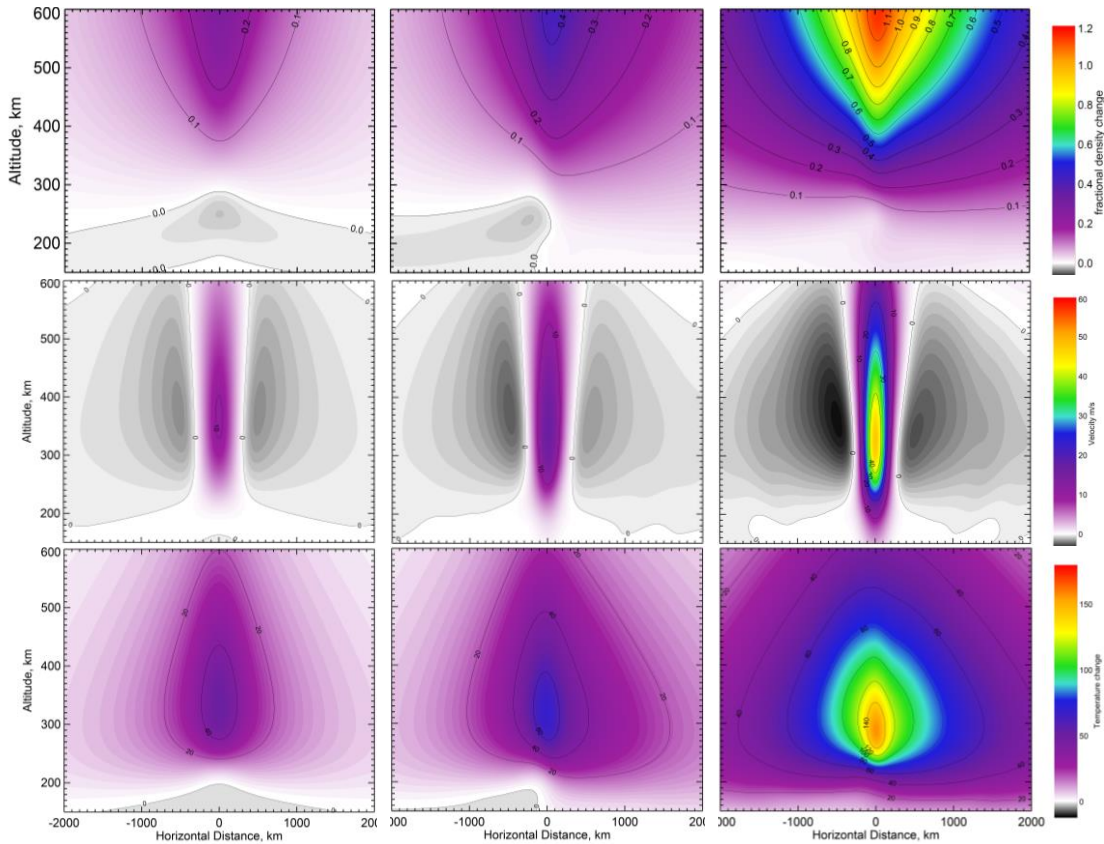


Figure 8. Fractional density change, vertical winds, and temperature change at 7200 s for a cusp latitudinal e-folding width of  $4^\circ$  with heating due to (a) particle precipitation only PPO case, (b) particle precipitation and Joule heating PEF1 case and (c) particle precipitation and Joule heating PEF2 case.

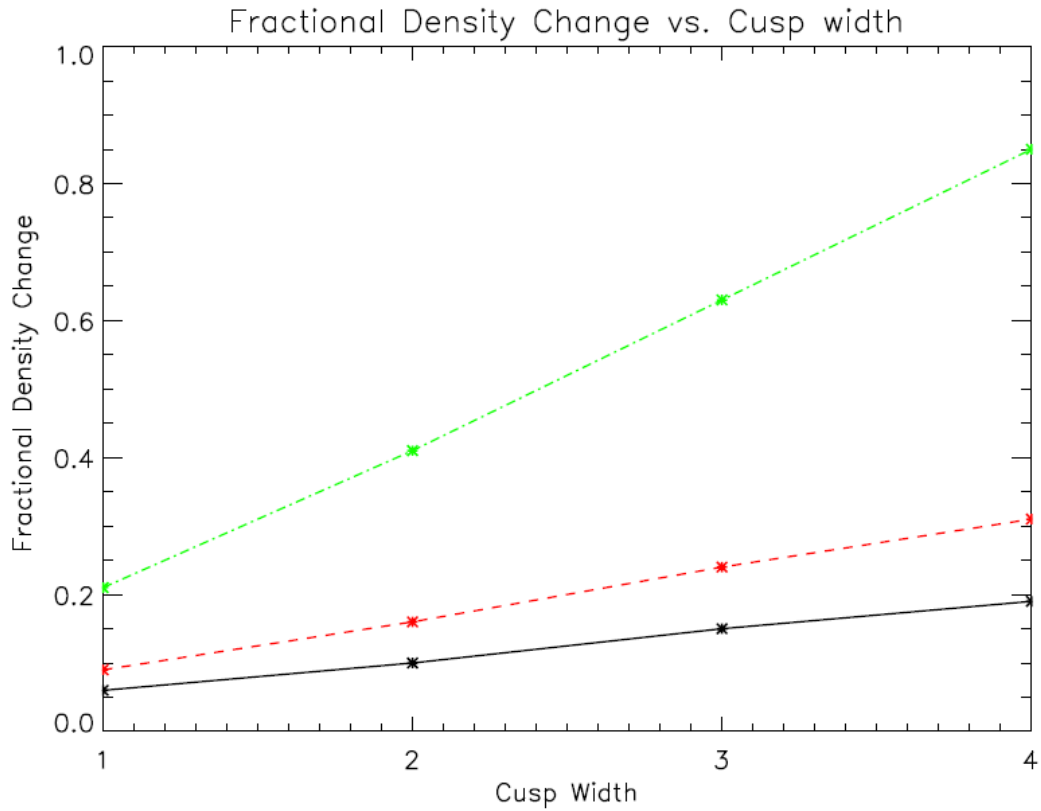


Figure 9. Fractional density change after 7200 s as a function of cusp width for particle heating only (solid black), case PEF1 (dashed red) and case PEF2 (dashed-dot green).

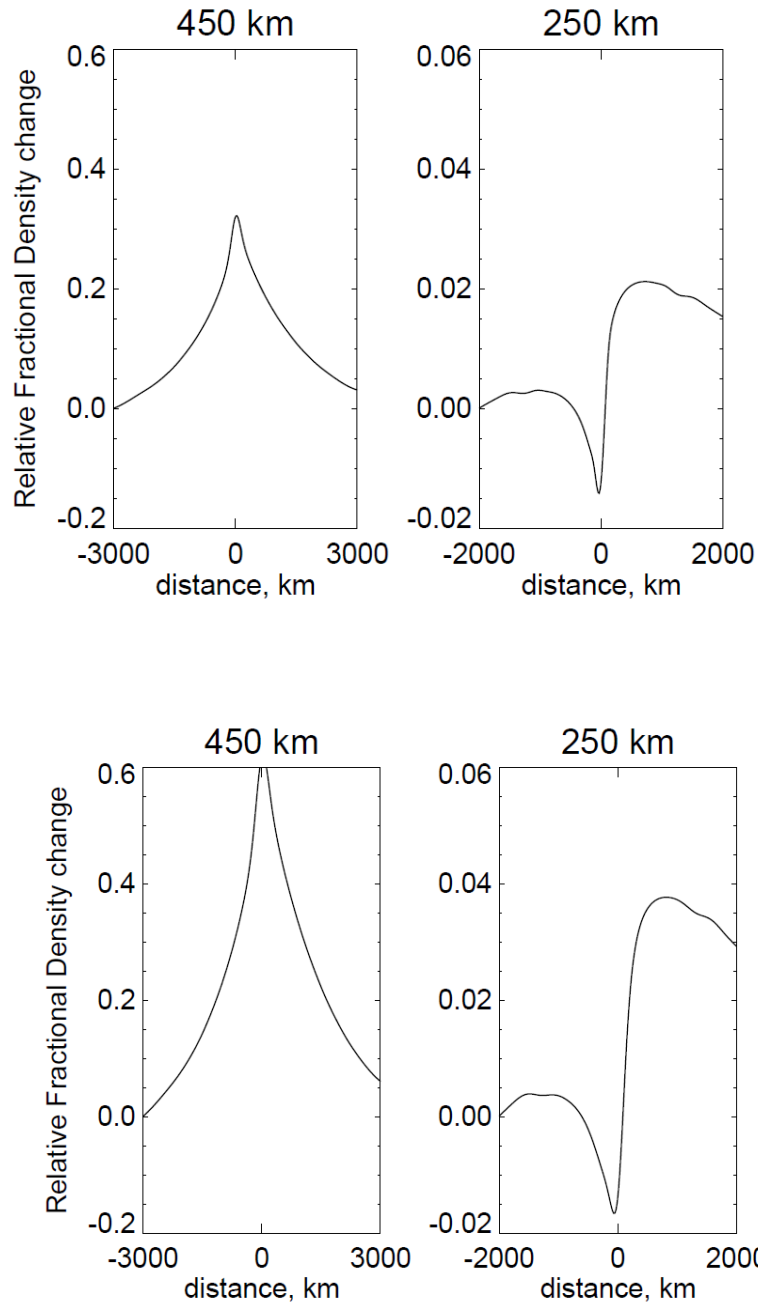


Figure 10. Variation of fractional density change after 7200 s along satellite tracks for the CHAMP (450 km) and Streak (250 km) satellites for case PEF2 for a 2° (top) width and a 4° cusp width (bottom). The density change is referenced to points outside of the cusp (density at the southernmost point plotted).

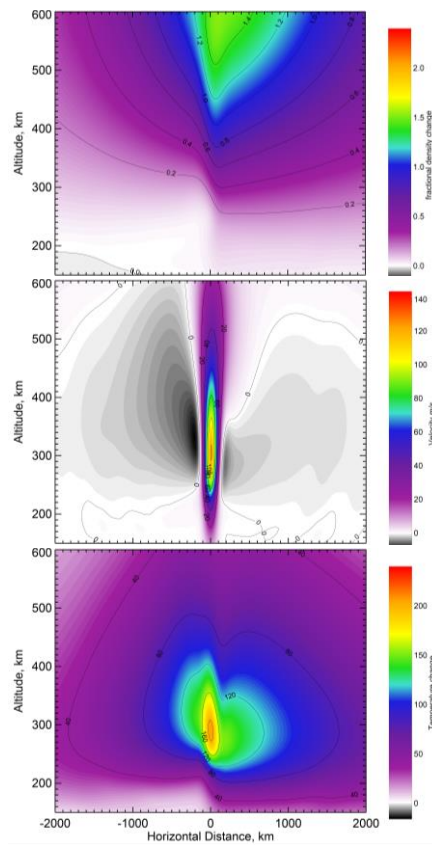


Figure 11. Fractional density change, vertical wind and temperature change versus altitude and latitude (horizontal distance) for a  $2^\circ$  cusp with particle heating PPO and elevated Joule heating with  $E_{dc} = 75$  mV/m and  $E_{ac} = 50$  mV/m.

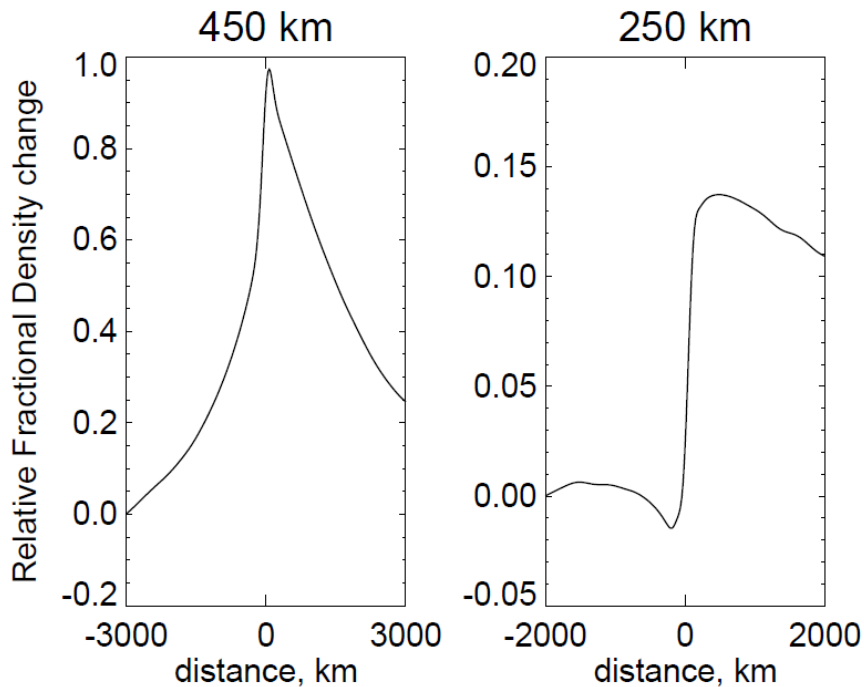


Figure 12. Variation of fractional density change after 7200 s along satellite tracks for the CHAMP (450 km) and Streak (250 km) satellites with a  $2^\circ$  width for the DC excursion case shown in figure 11. The density change is referenced to points outside of the cusp (density at the southernmost point plotted).